Prepared for ASME Symposium
on "Materials Problems in
Pressure Vessels", Nov. 17-22,
1963, Philadelphia, Pa.

CORRELATION OF UNIAXIAL NOTCH TENSILE DATA WITH PRESSURE-VESSEL FRACTURE CHARACTERISTICS

22 p.

By David L. Getz, William S. Pierce, and
Howard F. Calvert

Lewis Research Center
National Aeronautics and Space Administration
Cleveland, Ohio

ABSTRACT

This report presents experimental data of the fracture characteristics of aluminum 2014-T6 for ambient temperature, -321 F and -423 F. Correlation of the notched uniaxial tensile specimens and the pressure vessels is presented by a modification of the methods of Irwin and of Kuhn. A brief description of the cryogenic facilities is included.

INTRODUCTION

Many of the future boost- and space-vehicle systems, such as Nova, Saturn, Centaur, and vehicles using nuclear propulsion, will utilize hydrogen as a propellant in one or more of the stages. These space-vehicle systems require materials that have a maximum usable strength-to-weight ratio at temperatures down to -423 F. A basic design problem exists because of brittle fracture characteristics of most of the very high strength alloys. The ASTM Committee on Fracture Testing of High-Strength Sheet Materials has recommended the use of sharply notched uniaxial tensile specimens to determine the relative merits of the many alloys on a fracture-toughness basis. Although this procedure is valuable in screening materials, it does not provide all the information required to properly utilize the full capabilities of a material in an actual cryogenic pressure-vessel application.

Factors that require study before notched tensile data can be applied with confidence to pressure-vessel design include differences in stress state, width effects, curvature effects, and general scale effects. The reliable utilization of uniaxial data must, therefore, be augmented by a suitable correlation between the uniaxial data and the strength of actual space structures.

A research program is being conducted at the NASA Lewis Research Center to study the basic fracture behavior of materials at cryogenic temperatures and to examine several possible correlation procedures for predicting pressure vessel strengths. The information reported herein was obtained in a study of the aluminum alloy 2014 in the T6 condition. Sharply notched holes, as indicated in Fig. 1, having various radii and lengths were machined in tensile specimens and in cylinders. Ends were installed on the cylinders, the resultant pressure vessels or biaxial specimens were pressurized to failure, and the burst strengths were correlated with the strengths of the notched tensile specimens by means of a modified Irwin approach. Correlation was also attempted by means of a method developed by Kuhn through use of the ultimate strength and elongation of the material. The tests were conducted at room temperature, -321 and -423 F.

EXPERIMENTAL APPARATUS

Various types and sizes of biaxial specimens have been reported in the literature; however, after a thorough survey, it was concluded that a cylindrical specimen with removable and reusable ends would be the most practical and economical specimen for this research. By pressurizing the assembled pressure vessel to the burst point, the 2 to 1 stress field could be adequately studied. The following sections will describe

the biaxial and the uniaxial specimens, the end closures, and the test facility.

Test Specimens.

The biaxial and the uniaxial specimens were machined from extruded 2014-T6 aluminum tubing with tensile data as shown in the following table:

Tensile Data / Temperature	Ultimate Strength (psi)	Yield Strength (psi)	0.0002" Radius Notch Strength Net Section (psi)	0.0002" Radius Notch Strength Gross Section (psi)
Ambient	76,300	70,000	67,800	60,100
-321 F	93,900	81,900	77,000	68,000
-423 F	108,400	90,800	81,500	72,800

The chemical analysis showed an alloying content of 4.4 Cu, 0.36 Fe, 0.92 Si, 0.79 Mn, 0.42 Mg, 0.08 Zn, 0.01 Ni, 0.01 Cr, 0.03 Ti, and 0.01 Sn. Before heat treatment, 12-inch lengths of tubing were removed at regular intervals and were cut in half longitudinally and flattened. The remaining tubing and the flattened pieces were then heat treated to the T6 condition; therefore, all the specimens were made from the same heat of material and received the same heat treatment. The test section in both types of specimens was 0.060-inch thick. The notches were formed by drilling through with a No. 48 drill and then machining two notches diametrically opposite one another. Notch length was varied by first elongating the hole to the desired length and then machining the notches at the ends of the hole. The notch length was varied only in the biaxial specimens; the uniaxial specimens all had notches approximately 0.112 inch long. The uniaxial specimens were machined in accordance with

the specifications given in reference 1. Fig. 1 is a sketch of the uniaxial and biaxial specimens with an enlarged section showing the notch configuration and the orientation. The orientation of the notches was such that the maximum stress-concentration effect was in the direction of the maximum principal stress. The second insert shows a representative elongated notch in the cylinder.

The through notch in the biaxial specimen was sealed for pressurizing with a composite internal patch consisting of a layer of 0.002 mylar tape, a layer of 0.010 stainless-steel shim, and additional layers of overlapping mylar tape. It is believed that the patch did not add appreciably to the cylinder strength, nor did it affect the fracture mechanism.

Biaxial Specimen End Closures

The biaxial specimen selected for this research was a machined cylinder; therefore, end closures had to be provided to form a pressure vessel. Removable and reusable ends were developed. One end incorporated a special filler designed to reduce the volume of liquid in contact with the specimen and to be compatible with the unusual density characteristics associated with the pressurizing of liquid hydrogen with gaseous helium. At -423 F and at pressures less than approximately 600 psi, gaseous helium is lighter than liquid hydrogen; however, at pressures greater than approximately 600 psi, gaseous helium is heavier than liquid hydrogen. Fig. 2 shows a cross section of an assembled vessel. The specimen ends are locked into the removable heads by filling the tapered cavity with a low-melting-point alloy that expands as it cools. The helium gas can either be at the top

of the center tube or at the bottom as shown in the figure, and a continual supply of liquid hydrogen was supplied through the orifice to help ensure a hydraulic failure.

Test Facility

A research project utilizing liquid hydrogen as a test medium requires a specially designed facility. A typical NASA Lewis test cell is shown in Fig. 3 and is described in greater detail in reference 2. The general design criteria requires that the tests be conducted in open-air conditions. The cryostat containing the test specimen is shown in the center of the figure.

ANALYSIS OF EXPERIMENTAL DATA

Modified Irwin Method

The correlation of the fracture stresses of the uniaxial tensile specimens and the pressure vessels presented herein was tried by the use of two different methods. The first method requires an introduction to the work of Irwin (Ref. 3), who gives a criterion for the evaluation of fracture toughness. His method employs the theory of elasticity to give a single parameter characterization of the intensity of the stress field surrounding a crack tip in a structural member or a test specimen. Unstable crack growth is supposed to occur when the stress-intensity factor K reaches a level characteristic of the material known as the fracture toughness K_c.

The effect of local stress relaxation due to plastic flow near the end of the crack tip in a ductile material is considered to be sufficiently approximated by an effective increase in the critical crack length at the moment of fast fracture. The magnitude of the increase, called the

plastic zone correction, is estimated to be the square of the ratio of K_c to the yield strength divided by 2π. Thus, Irwin arrived at the following relationship for K_c of a finite-width uniaxial center-notched tensile specimen:

$$K_c = \sigma \left[w \tan \frac{\pi}{w} \left(a + \frac{K_c^2}{2\pi\sigma_{YS}^2} \right) \right]^{1/2} \tag{1}$$

where

σ gross section fracture stress

w gross width of specimen

a 1/2 of the central crack length at the moment of fast fracture

σ_{YS} uniaxial yield stress

$\frac{K_c^2}{2\pi\sigma_{YS}^2}$ uniaxial plastic-zone correction term

When applied to wide specimens where a/w is very small, the above equation can be rewritten as

$$\sigma = \frac{K_c}{\sqrt{\pi \left(a + \frac{K_c^2}{2\pi\sigma_{YS}^2} \right)}} \tag{2}$$

In the correlation used herein, the uniaxial plastic-zone correction term of Irwin's equation was left open for experimental modification for the biaxial stress state of a pressure vessel by the parameter of correlation b_G. Thus, the correlation equation, using the Irwin method as a basis, takes the following form:

$$\sigma_H = \frac{K_{C_N}}{\sqrt{\pi\left(a_o + \frac{b_G K_{C_N}^2}{2\pi\sigma_{YS}^2}\right)}} \tag{3}$$

where

σ_H hoop fracture stress

K_{C_N} uniaxial-stress field-intensity parameter computed from equation (1) by replacing a with a_o

a_o 1/2 the initial length of the machined notch

b_G parameter of correlation

σ_{YS} uniaxial yield stress

Strict adherence to the Irwin method requires the evaluation of K_c by the observation of the maximum load and the crack length at the moment of unstable crack growth. In the correlation presented herein, it was assumed that the slow (or stable) crack growth was the same for both the tensile specimens and the pressure vessels and could, therefore, be neglected. In so doing, the crack length at the moment of unstable crack growth was taken as the initial dimensions of the machined notch; hence, the notation K_{C_N}.

In addition, it was assumed that the combined effects of stress state and curvature are reflected by the correlation parameter b_G. The effect of specimen width is contained in the expression for K_{C_N}.

Kuhn Method

The second method, proposed by Kuhn (Ref. 4) predicts the effect of

a notch or crack on the fatigue and static strength of a uniaxial tensile specimen or a pressure vessel. It is assumed that the failure of the part occurs when the peak stress in the net section becomes equal to the ultimate strength of the material.

This method employs the theory of elasticity to express the theoretical stress-concentration factor resulting from a tensile-stress field in an infinite sheet containing an elliptical hole. The resulting relationship is

$$K_T' = 1 + 2\sqrt{\frac{a}{\rho}} \tag{4}$$

When applied to a slender elliptical notch, a is 1/2 the initial notch length, and ρ is the notch radius.

The stress concentration factor is then corrected for the various physical effects present, most of which are evaluated by correlation with experimental data. First, the theoretical stress analysis is corrected for the effect of finite specimen width by the finite width factor K_w (verified by photoelasticity) as follows:

$$K_T = 1 + 2K_w\sqrt{\frac{a}{\rho}} \tag{5}$$

where

$$K_w = \sqrt{\frac{1 - 2a/w}{1 + 2a/w}}$$

and w is the specimen width.

The second correction is caused by the size effect that is exhibited by materials with granular structure when stress gradients are present. The expression shown below for this correction contains a quantity ρ' termed a "Neuber constant" and presumed to be a material property.

$$K_N = 1 + \frac{K_T - 1}{1 + \sqrt{\frac{\rho'}{\rho}}} \tag{6}$$

Values of ρ' can be obtained from either notch fatigue tests or static tests on notched or cracked specimens. For wrought aluminum alloys, however, Kuhn found that the ρ' values derived from fatigue tests were the same as those of static tests. Also, the ρ' values could be represented as a function of the ultimate tensile strength of the material.

The third correction is for the effect of plasticity represented by the following relationship:

$$K_P = 1 + (K_N - 1)\frac{E_1}{E} \tag{7}$$

where

E_1 secant modulus pertaining to the peak stress at the root of the notch

E Young's modulus

The ratio E_1/E can be estimated by the following empirical relationship applicable to aluminum alloys:

$$\frac{E_1}{E} \approx \frac{1}{1 + \frac{0.8eE}{\sigma_u}} \tag{8}$$

where

e elongation measured on the standard 2-inch gage length

E Young's modulus

σ_u ultimate tensile strength

Next, Kuhn relates the distinction between specimens with cracks and those with finite radius notches by a flow-restraint factor B determined

empirically as a function of K_T. The correction is applied to K_P as follows:

$$K_u^* = \frac{K_P}{1 + B} \tag{9}$$

This factor describes the increase in ultimate strength found in notched specimens of sizable notch radius due to the effect of the high-stress gradient present. The much lower stressed material slightly removed from the notch root restrains plastic flow at the root resulting in notch strengthening effects.

A final curvature correction is necessary for a longitudinal notch in a cylindrical pressure vessel. The correction determined for aluminum alloys is empirical and relates the stress concentration factor in a cylinder with that of a corresponding flat tensile specimen as follows:

$$K_{u_{(cyl)}} = K_u^* \left[1 + 5\left(\frac{2a}{R}\right)\right] \tag{10}$$

where

2a total length of longitudinal notch

R radius of the cylinder

The final result is a stress-concentration factor relating the average hoop-fracture stress acting on the net section with the ultimate strength of the material as follows:

$$\sigma_H = \frac{\sigma_u}{K_{u_{(cyl)}}} \tag{11}$$

RESULTS AND DISCUSSION

Temperature - Notch-Radius Study

The validity of the two correlations outlined was examined by the introduction of the effects of temperature, notch radius, and notch length. The

temperature - notch-radius study at a constant notch length of approximately 0.112 inch was analyzed by two treatments of the data as shown in Fig. 4. The first treatment determined the values of b_G for each of the three temperatures by substituting into Eq. (3) the corresponding experimental values of σ_H and K_{C_N} for the notch radius of 0.0002 inch. This radius simulates a natural crack more closely than do the larger radii. The resulting b_G values were then held constant for the predictions of σ_H for the larger radii notches. The unique values of K_{C_N}, however, were used; i.e., if the predicted σ_H for a 0.001-inch-radius notch was desired, it was computed from Eq. (3) by the insertion of the value of K_{C_N} determined from a tensile specimen having 0.001-inch radius notch. The value of b_G was a constant for the temperature of interest.

The statistical treatment used (see appendix A) inherently accepts the influence of the data of all three radii in determining the correlation parameter b_G for a particular temperature. The statistical treatment caused the predicted curves to plot as straight lines (see Fig. 4). Note that the statistical values of b_G differed slightly from those determined from only the 0.0002-inch radius data. The statistical values of b_G for cryogenic temperatures (Table I, appendix A) indicate the decreasing trend with lower temperatures and lower notch radii; all values remain less than unity. This could be a physical indication that b_G is truly a measure of the change of the plastic zone size.

The correlation parameter term b_G, does not appear in Irwin's equation (Eq. (1)) for tensile specimens because it is equal to unity.

For the temperature - notch-radius study shown in Fig. 4 (notch lengths of 0.112 in.), a value of b_G equal to unity would cause the predicted values of σ_H to be 10 percent lower (7000 psi) at -321 F and 12 percent lower (10,000 psi) at -423 F for a 0.0002-inch radius notch.

Kuhn's method was also applied to the temperature - notch-radius study, but with limited success. The predicted burst stresses were 13 - 24 percent low at ambient temperature, 1 - 13 percent low at -321 F, and 6 - 18 percent low at -423 F.

Temperature - Notch-Length Study

The values of b_G determined by the temperature - notch-radius study were used in an extrapolation of the correlations to higher notch lengths in the pressure cylinders for the temperatures of -321 F and -423 F and for a notch radius of 0.0002-inch (Figs. 5 and 6). The extrapolations for both temperatures appear to be good predictors of the effects of notch lengths up to 0.750 inch. Above 0.750 inch the extrapolations are overly optimistic, and the extrapolation curves are not significantly affected when a value of b_G equal to unity is used. A possible explanation is the change of crack surface-displacement mode that caused a deviation of the K_C values. Examination of the fracture surfaces showed unidirectional oblique shear failure indicative of a transverse shear mode of crack extension, - in other words, a tearing action caused by the bulging cylinder wall. After fracture, the material on one side of the longitudinal fracture was more radially deflected than the other. Consequently, overlapping of the two surfaces occurred, which provided evidence of tearing action.

The effect of a tenfold increase of notch radius of 0.002 inch for notch lengths of 0.250 inch and greater was examined at -423 F (Fig. 6). The effect was insignificant; the aluminum alloy tested is not extremely notch sensitive at -423 F. Consequently, variations in notch radius do not significantly affect the fracture stress. With more notch-sensitive materials, however, the effect of notch radius would probably be significant.

The method of Kuhn computed for a 0.0002-inch-radius notch is in close agreement with the test data at notch lengths exceeding 0.750 inch. The method of Kuhn also predicts that the hoop-fracture stress reaches the ultimate tensile strength as the notch length approaches zero. This prediction was found to be accurate for the unnotched cylinders tested. In the range of notch lengths between zero and 0.750 inch, however, Kuhn's method gives low predictions (i.e., 23 percent for a 0.250-in. notch at -423 F).

CONCLUDING REMARKS

The two separate correlations presented are an attempt to relate the fracture characteristics of a model notched pressure vessel to those of a notched flat tensile specimen. The correlations are not meant to explain the phenomenon of brittle fracture, but rather to examine the value of two promising methods available for design usage. Since the examination is a limited one, no conclusions can be drawn for other specimen geometries, loadings, or materials. The results, however, do show the possibility of bridging the present knowledge gap of the fracture process by semi-empirical expressions determined by experimental results. Also, the data

presented will always have great value when helping to accept or to reject any future hypotheses concerning the fracture process.

APPENDIX A

The statistical treatment used was based on the analysis of variance technique (Ref. 5, ch. 10). Variance is a measure of deviation, and when it is supplemented with the arithmetic mean, a clear picture of a distribution is known. Analysis of variance determines whether the effects introduced produce real effects or effects of a random nature. The relative magnitude of all effects producing a difference between any single measurement and the grand mean of all the measurements can then be compared as components of variance. The original measurements can be adjusted to the expected values that are the average values, which one would obtain if an infinite number of measurements or tests were made. An outline of the computational procedure follows. The experimental data of K_{C_N} and σ_H values were first arranged in a fixed-effects crossed model table using the two categories of temperature and notch radius.

TEMPERATURE EFFECT
(b categories, index j)

NOTCH RADIUS EFFECT
(a categories, index i)

	Ambient	-321 F	-423 F	
0.0002"	X_{ijk} } n tests index, k Avg. $\bar{X}_{ij.}$			Mean of rows $\bar{X}_{i..}$
.001"				
.005"				
	Mean of columns $\bar{X}_{.j.}$			Grand mean $\bar{X}_{...}$

Three measurements were taken for each cell; each measurement or test indexed by the notation X_{ijk} (the mean of the cell $\bar{X}_{ij.}$). Each row has the mean $\bar{X}_{i..}$, each column $\bar{X}_{.j.}$, and the grand mean is $\bar{X}_{...}$.

The measure of the continued effects present are represented by the following summations:

Notch radius + randomness

$$\frac{nb\sum_{i}(\bar{X}_{i..} - \bar{X}_{...})^2}{(a-1)} = M.S._R$$

Temperature + randomness

$$\frac{na\sum_{j}(\bar{X}_{.j.} - \bar{X}_{...})^2}{(b-1)} = M.S._T$$

Interaction + randomness

$$\frac{n\sum_{i}\sum_{j}(\bar{X}_{ij.} - \bar{X}_{i..} - \bar{X}_{.j.} + \bar{X}_{...})^2}{(a-1)(b-1)} = M.S._{RT}$$

Randomness

$$\frac{\sum_{i}\sum_{j}\sum_{k}(X_{ijk} - \bar{X}_{ij.})^2}{ab(n-1)} = M.S._{\epsilon(RT)}$$

To determine whether notch radius, temperature, or interaction introduce significant effects, the F ratios $\frac{M.S._R}{M.S._{\epsilon(RT)}}$, $\frac{M.S._T}{M.S._{\epsilon(RT)}}$, and $\frac{M.S._{RT}}{M.S._{\epsilon(RT)}}$ are each compared with their F statistic for the appropriate degrees of freedom and levels of significance. The use of this statistic

has been justified mathematically correct for normal populations. The magnitude of randomness is evaluated by a sample size of three specimens in each cell. The other significant combined effects, therefore, can be separated into the effects of notch radius and temperature; interaction was not found to be significant. These effects are compared as components of variance on a percentage basis.

The data were adjusted to expected values by use of the t distribution and application of the criteria of $\bar{X}_{...}$ ±3 standard deviations to either correct the means of the rows and columns to the grand mean or to allow the means to retain their distinct identity. The expected values of the cell means were then calculated by the following equation: $\bar{X}'_{ij.} = \bar{X}'_{i..} + \bar{X}'_{.j.} - \bar{X}_{...}$ where the primes denote expected values.

Table II gives the components of variance for K_{C_N} (an indicator of uniaxial fracture stress) and σ_H (the actual hoop-fracture stress). In both measurements the temperature effect was greater than the notch radius effect; for the pressure vessels, the temperature effect was over ten times the notch-radius effect. The randomness present in the measurement of K_{C_N} was over ten times that of σ_H. It may possibly be explained that since the desired notch radius is more difficult to accurately obtain than the desired temperature, the determination of K_{C_N} will then naturally experience more randomness than σ_H because K_{C_N} is more affected by notch radius than σ_H. The fact that the distinct specified radii were more easily and accurately machined in the tensile specimens than in the pressure vessels provides another explanation.

REFERENCES

1) Hanson, M. P., Stickley, G. W., and Richards, H.T.: "Sharp-Notch Behavior of Some High-Strength Sheet, Aluminum Alloys and Welded Joints at 75°, -320°, and -423° F." Spec. Tech. Pub. 287, ASTM, May 1960.

2) Calvert, H. F., and Kemp, R. H.: "Determination of Pressure Vessel Strengths at -423° F as Influenced by Notches of Various Radii," Paper presented at SAE, Apr. 1962.

3) Irwin, G. R.: "Fracture Testing of High-Strength Sheet Materials Under Conditions Appropriate for Stress Analysis," N.R.L. Rep. 5486, July 27, 1960.

4) Kuhn, Paul: "Notch Effects on Fatigue and Static Strength," Paper presented at Symposium on Aero. Fatigue, Rome, Italy, Apr. 1963.

5) Dixon, W. J., and Massey, F. J., Jr.: "Introduction to Statistical Analysis," Second ed., McGraw-Hill Book Co., Inc., 1957.

TABLE I. - STATISTICAL b_G VALUES SHOWING THE TEMPERATURE-NOTCH RADIUS TRENDS

Notch radius, in.	b_G		
	Ambient	-321 F	-423 F
0.0002	0.68	0.51	0.36
.001	.67	.54	.42
.005	.68	.59	.47
Averages used in correlation	0.68	0.55	0.42

TABLE II. - RELATIVE MAGNITUDE OF SIGNIFICANT EFFECTS PRESENT IN THE TEMPERATURE-NOTCH RADIUS STUDY

Effects Present	K_{C_N} (percent)	σ_H (percent)
Temperature	34	88
Notch radius	24	8
Randomness	42	4
Total	100	100

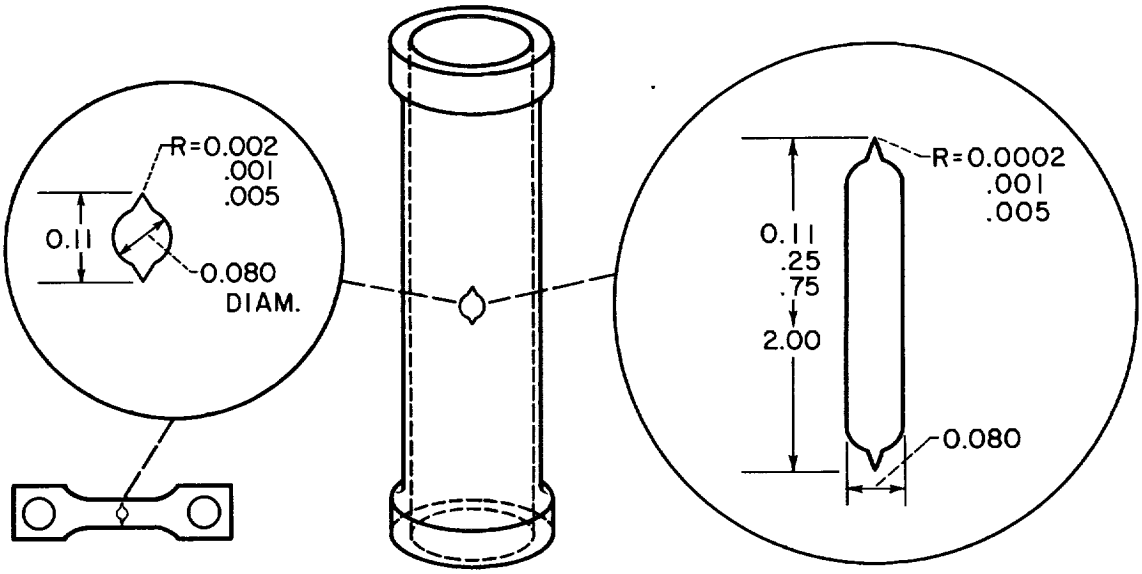

Fig. 1 Notch configuration and orientation in uniaxial and biaxial stress specimens.

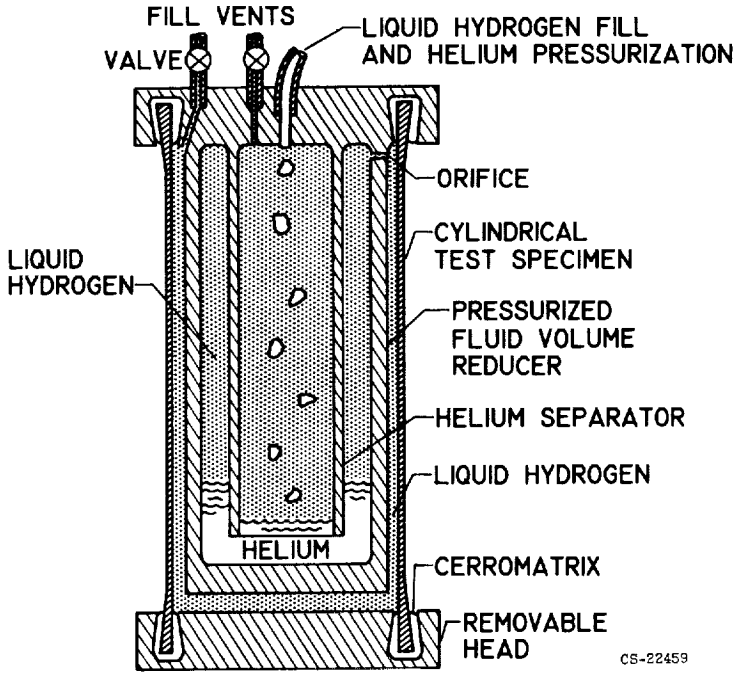

Fig. 2 Specimen holder for low-cost biaxial testing at cryogenic temperatures.

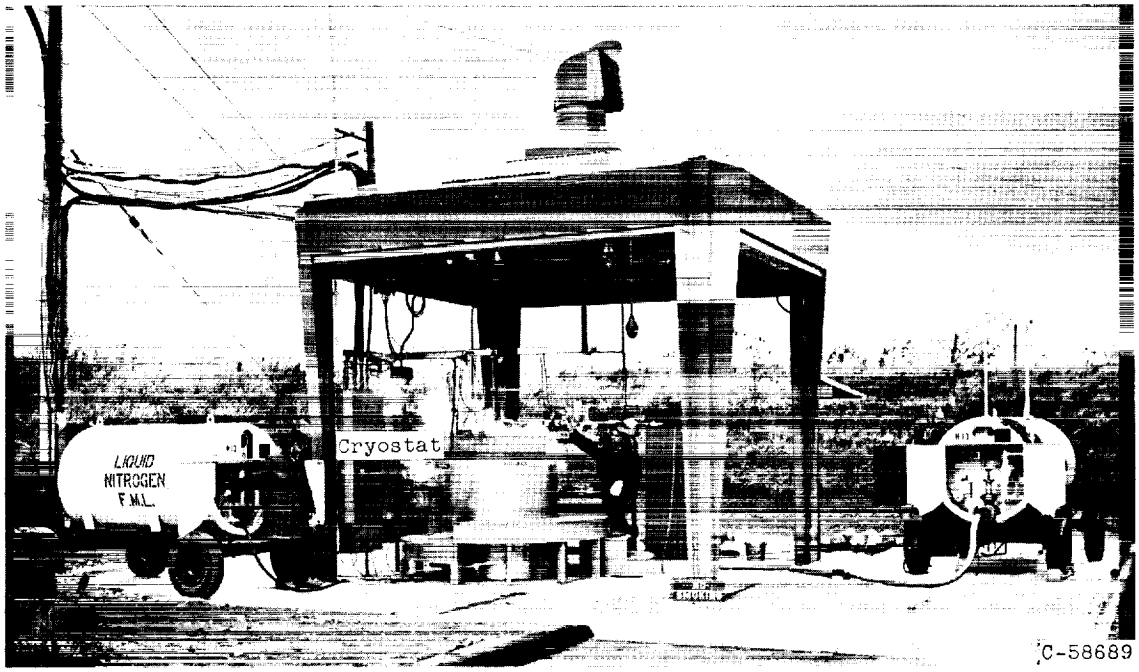

Fig. 3 Test cell for bursting pressure vessels filled with liquid hydrogen.

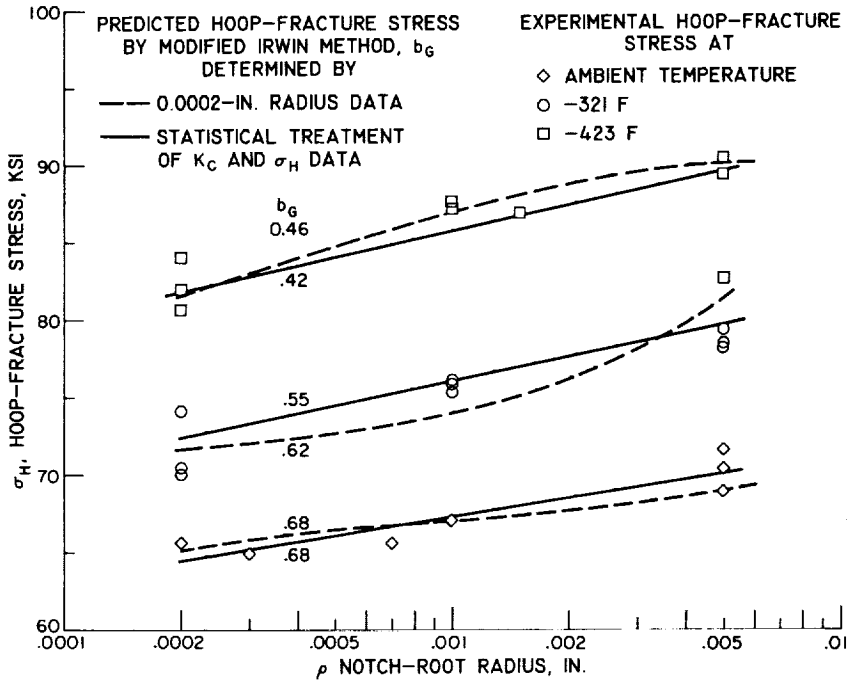

Fig. 4 Correlation by the parameter b_g of uniaxial tensile specimens and pressure vessels containing notches of various radii.

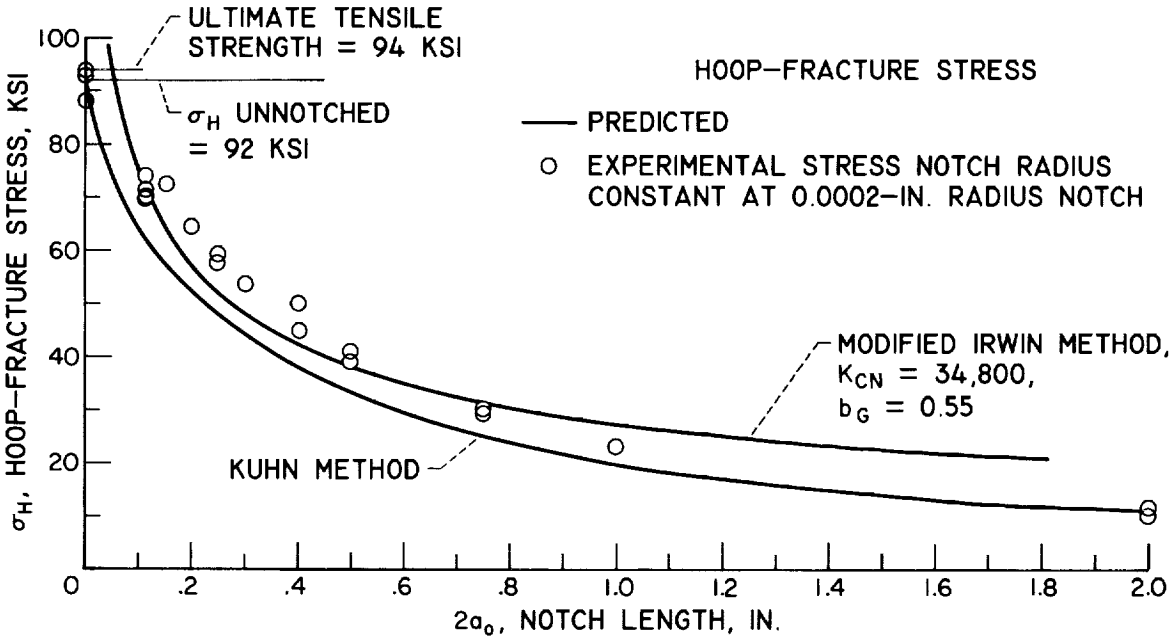

Fig. 5 Extrapolation with b_g to correlate various notch lengths at -321 F.

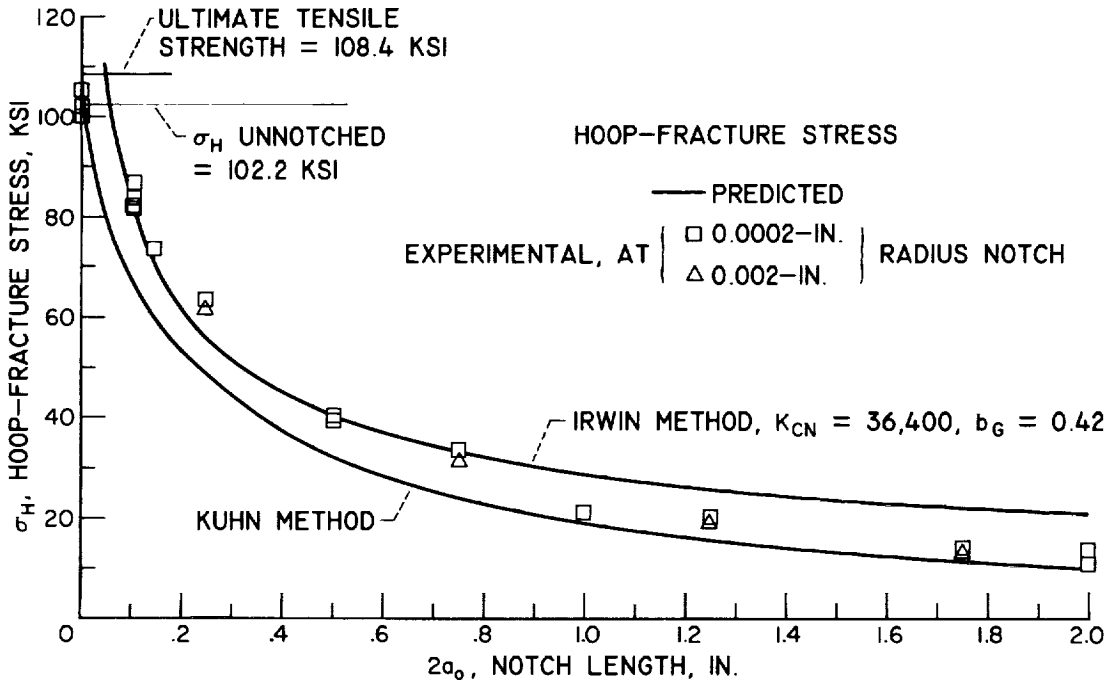

Fig. 6 Extrapolation with b_g to correlate various notch lengths at -423 F.